IJE TRANSACTIONS B: Applications Vol. 34, No. 05, (May 2021) 1321-1328

International Journal of Engineering

Journal Homepage: www.ije.ir

# Finite Element Simulation and Experimental Test of Ovine Corneal Tissue Cutting Process in Cataract Surgery Operation

H. Band Band[a], M. Arbabtafti*[a], A. Nahvi[b], M. Zarei-Ghanavati[c]

[a] *Department of Mechanical Engineering, Shahid Rajaee Teacher Training University, Tehran, Iran*
[b] *Department of Mechanical Engineering, K.N. Toosi University of Technology, Tehran, Iran*
[c] *Department of Ophthalmology, Tehran University of Medical Sciences, Tehran, Iran*

*PAPER INFO*

*Paper history:*
Received 09 December 2020
Received in revised form 13 March 2021
Accepted 09 April 2021

*Keywords*:
*Finite Element Model*
*Corneal Cutting Force*
*Soft Tissue Damage Model*
*Corneal Surgery Modeling*
*Needle Insertion*

*ABSTRACT*

The modeling of corneal tissue cutting is essential in developing haptic training simulators and robot-assisted surgeries. A finite element model was developed in this study for the ovine corneal cutting process and validated with an experimental setup for the first time. The experimental setup forces are measured in pre-cutting, cutting, and relaxation phases. The mechanical behavior of corneal incision was modeled by the finite element method. A test setup was built to conduct experiments on 32 fresh and well-preserved ovine cornea. Force was recorded with the sampling rate of 200 Hz. The tests were performed for intraocular pressures from 15 mm-Hg to 18 mm-Hg, and keratome velocities of 1 mm/s and 2 mm/s. The finite element model characterized the nonlinear behavior of the ovine corneal tissue. In the pre-cutting phase, the force is increased until the instrument tip penetrates. A 12.3% (2 mm/s) and 19.1% (1 mm/s) reduction in force indicated the onset of the cutting phase after which force remained constant. At the relaxation phase, force returned to zero. The cutting force values varied by pressure between 0.183N and 0.287 N for 1 mm/s and between 0.211 N and 0.281 N for 2 mm/s of keratome velocity, respectively. The finite element simulations show that the maximum force errors predicted by the model is 0.042 N for 2 mm/s of keratome velocity. The root mean square of force error between the finite element simulations and the experiments is 0.025 N.

***doi**: 10.5829/ije.2021.34.05b.27*

## 1. INTRODUCTION

Cataract surgery simulations are useful for training surgeons and to administer surgery via teleoperation. Finite element method (FEM) can be used to model corneal mechanical behavior when subjected to internal and external forces [1]. There are a few valuable research works in the literature investigating the finite element (FE) models of the cornea under various types of loading, but the FEM of the corneal cutting procedure during cataract surgery is not adequately studied yet. Experiments on the corneal tissue can greatly help researchers understand the mechanics of deformation and rupture during cataract surgery and develop valid FE models. In previous studies, a few types of FE models of cornea have been presented. Also, there are some research works on FE models of needle insertion. These FE models can be broken down into three main categories including corneal surgery, corneal impact, trauma, and needle insertion into soft and artificial tissues. FE models of corneal surgeries, impacts and trauma are somehow comparable to the FE simulation of cataract surgeries. However, none of these FE models has addressed cutting of the corneal tissue. The most relevant simulations of cataract surgery operation are needle insertion experiments and FE simulations.

FE model of refractive surgery and corneal deformation has been developed to plan surgical procedures and predict corneal mechanical properties. The curvature of the corneal surfaces affects its refractive power significantly. Refractive surgery is used to improve the visual acuity of patients with common

*Corresponding Author Institutional Email: arbabtafti@sru.ac.ir (M. Arbabtafti)

Please cite this article as: H. Band Band, M. Arbabtafti, A. Nahvi, M. Zarei-Ghanavati, Finite Element Simulation and Experimental Test of Ovine Corneal Tissue Cutting Process in Cataract Surgery Operation, International Journal of Engineering, Transactions B: Applications Vol. 34, No. 05, (2021) 1321-1328

refractive illnesses. FEM has been used to analyze mechanical properties and corneal curvature before and after the refractive surgery [2-9]. Moreover, an FE model has been developed for simulating corneal tissue cutting by using boundary condition [10]. The FE model has been employed to compare and revise nomogram tables or graphics used by surgeons to plan surgical procedures [11, 12]. In other studies, a 3-D FE model has been used to compare the results of small-incision and LASIK operations [13]. Additionally, FE simulation has been used to correct astigmatism [14]. Moreover, a 3-D FE model has been used to study the accommodation behavior of crystalline lens after Femtosecond (FS) laser treatment [15]. Additionally, a 3-D FE simulation has been used to investigate the deformation of cornea during tonometry [16]. However, none of these FE models concerns the cutting process of the corneal tissue.

FEM has been employed as a useful and inexpensive tool for simulating ocular injuries and bringing solutions to reduce eye injuries. In these types of studies, factors such as velocity, mass, material, and size of the projectile have been taken into account [17-19]. Additionally, FE simulation of rupture of corneal tissue due to airbag injuries has been developed [20-21].

The FE model of needle insertion has been developed to determine needle forces during soft tissue cutting. Two-dimensional FE model of needle insertion has been developed to predict needle deflection, and also for steering the needle towards soft tissue in robotic systems [22]. FEM can be used for needle–tissue interactions by simulating material properties, material rupture, large deformation, and boundary conditions [23]. A FE simulation with cohesive zone model can be used to investigate tip rupture [24-25]. However, a cohesive zone algorithm requires a priori needle route. FE model has also been used to simulate needle-tissue interaction forces with an element deletion-based method [26-27]. In these studies, a micro-needle was inserted into a 2D and 3D multilayer skin model.

This paper presents an experimental setup for simulating the first step of cataract surgery operation by recording cutting force of the ovine corneal tissue for the first time. The effect of intra-ocular pressure and surgeon's hand velocity on the incision force was investigated. Moreover, a FE simulation of the ovine corneal tissue cutting process was developed based on the nonlinear behavior of the corneal tissue and it was validated experimentally.

The remaining of the paper is organized as follows. In section 2, we describe the experimental setup and the FE model. In the results section, we compare the corneal experimental results with those of the FE simulations. Finally, the paper is concluded by discussing the effect of the cutting force and repeatability of the tests.

## 2. MATERIALS AND METHODS

**2. 1. Experiments** The experimental setup was designed to penetrate the keratome inside the corneal tissue and record position, velocity, and force (see Figure 1). This setup simulates the cataract surgery operation with any desired penetration velocity. The setup allows adjustment of intraocular pressure, and keratome motion velocity during the incision process. The aim was to use a keratome to penetrate the soft tissue with a constant velocity while monitoring the force of cutting the tissue exerted on the keratome during the incision process.

Other experimental apparatus studies include needle insertion of prostate brachytherapy procedures [25, 28], needle insertion into an artificial material [29-30], needle insertion into agar gel by using three types of copper needle with bevel tips [31-32], and needle insertion into porcine cardiac tissue [33]. This paper models operation of the keratome tool on corneal tissue during cataract surgery .

The equipment consists of a keratome incision instrument, a data-acquisition card, a high-speed 120 frames per second camera, a linear potentiometer, a load cell, and a personal computer. The entire incision mechanism stands on a base and fixed with vertical

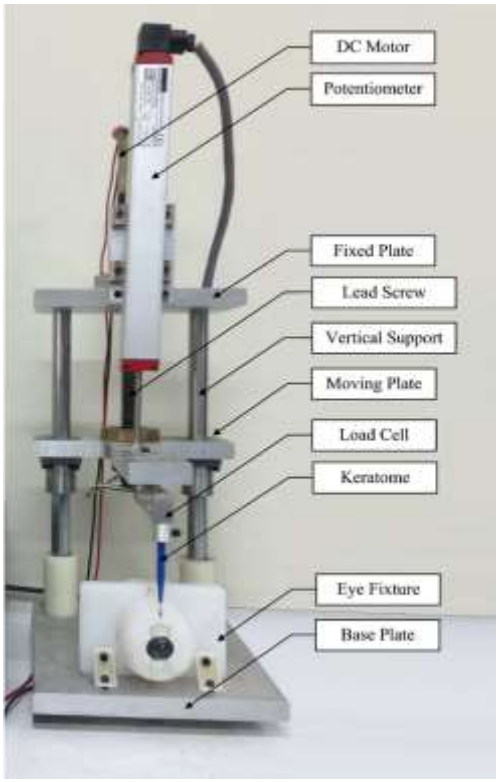


**Figure 1.** The test devices and equipment of cataract surgery mechanism

supports. A lead screw rotate by using a geared DC motor and the change of moving plate position measured by potentiometer (Opkon LPT 225 D 5K); also, a one axis force sensor (Scaime AR0.2 serial number 001503) fixed on moving plate and the keratome was screwed to the force sensor. The force sensor was fixed on an aluminum plate with one side attached to the anti-backlash nut traveling along the lead screw and the other side to a guiding shaft with a linear bearing to reduce friction of travel. The design and fabrication of the cutting assembly ensured that the system was sufficiently rigid. Accordingly, the forces recorded by the force sensor were those obtained by cutting the tissue alone like real forces, acting on the surgeon's hand during the cataract surgery operation.

To match the recorded values from the test and incision procedure, find the meaning of each variation in numerical values of the recorded force and tissue deformation, a high speed camera system was employed during the surgery simulation. The camera was placed close to the experimental setup to record scenes of the incision and tissue deformations step by step for later analysis. This consideration was made for recognition and accommodation of the force-time values with the steps of corneal tissue incision.

An experimental test was performed to record reaction forces to the surgeon's hand during the cataract surgery and use these forces for evaluating the finite element simulation. These forces play a substantial role in specifying the pattern of incision and defining the failure criteria of the cornea soft tissue. In light of this, 32 ovine eyes, because of their similarity to human eyes [34], and as it is the most practical choice of cataract surgery for trainers in wet labs in the Middle East and Central Asia [35], were used and prepared for the test within 4 hours of post-mortem. Since the experiments were implemented on the ex-vivo corneal tissue, the preparation procedure of the corneal tissue before the experiment helped maintain the properties of the tissue as close as to the in-vivo corneal tissue properties. The eyes were placed in an eye fixture during the implantation of the test, the design of which was inspired from previous studies [36], with some changes based on test situation. Finally, the test was repeated four times for each scenario. The effect of keratome motion velocity and intraocular pressure was considered.

The preceding pictures in Figure 2 present the penetration of keratome into the corneal tissue step by step. As it is obvious in this figure, the yellow lines show the edge of instrument while the red line shows the width of cutting.

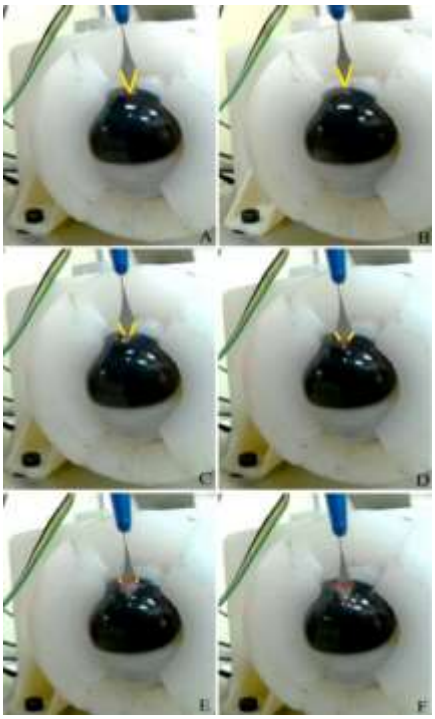

**Figure 2.** Keratome penetration into the cornea. A: Initial contact. B: deformation. C: initial cutting, D: cutting process. E: cutting process. F: complete pass of Keratome

**2. 2. Finite Element Analysis** A validated computational model can describe the incision process and predict the mechanical behavior of the cornea during incision. An FE model provides a quantitative estimation of the corneal tissue deformation resistance both before and during the incision process. This model iteratively solves for the characterizing parameters of the corneal soft tissue failure criterion.

The FE model determines the keratome-tissue interaction and the resulting forces applied by the surgeon's hand during operation. A three-dimensional FE model of the eye using 81771 linear hexahedral elements of type 8-node linear brick, including 2193 elements with average size of 1mm in region A, 54000 elements with average size of 0.52mm in region B associated with the location of incision, and 390 elements with average size of 0.54mm in region C, and also keratome with 186 linear hexahedral elements with average size of 0.36mm, was developed to simulate the first step of cataract surgery operation as shown in Figure 3.

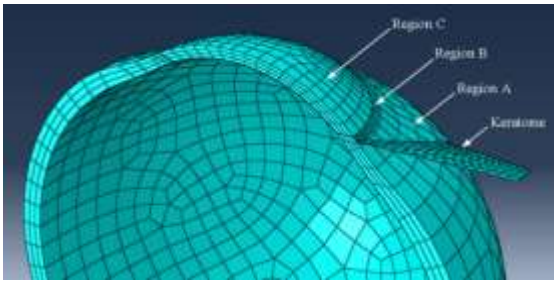


**Figure 3.** FE model of the eye and the keratome

The FE analysis was conducted with the ABAQUS finite element software using the VUMAT subroutine. The corneal tissue has non-linear behavior and its Young's modulus increases during deformation [34]. A constitutive model was used to demonstrate the exponential effect of the strain on the material's stress–strain behavior as obtained experimentally. In this consideration, a non-linear constitutive model was adopted from earlier studies [34]:

$$\sigma = a(e^{b\varepsilon} - 1) \quad (1)$$

where $a$ is equal to 0.22 MPa and $b$ is dimensionless and equal to 32.88. The Young's modulus is extracted from the first derivative of σ with respect to ε:

$$E = \frac{d\sigma}{d\varepsilon} = abe^{b\varepsilon} \quad (2)$$

The strain $\varepsilon$ is replaced by the equivalent strain $\varepsilon_{eq}$ obtained from the principal strains $\varepsilon_1$, $\varepsilon_2$ and $\varepsilon_3$:

$$\varepsilon_{eq} = \frac{2}{3}\sqrt{(\varepsilon_1 - \varepsilon_2)^2 + (\varepsilon_2 - \varepsilon_3)^2 + (\varepsilon_3 - \varepsilon_1)^2} \quad (3)$$

Defining this type of material behavior as the corneal tissue, as well as simulating the incision step and cutting the cornea is not possible in ABAQUS CAE. We developed a user-defined material model (VUMAT) FORTRAN subroutine to implement the material behavior of the corneal soft tissue and soft tissue cutting. For simulating the damage of the soft tissue by keratome incision, the explicit solver is more efficient and convergence of the solution in the explicit solver is easier compared to the implicit solver. In this analysis, a modified Johnson-Cook model and an element deletion-based method were used [17]. The damage behavior was implemented into ABAQUS via a VUMAT in conjunction with the non-linear elastic model. The modified Johnson-Cook model is simplified to the Von Misses stress as below:

$$\sigma = A \quad (4)$$

Which $A$ is a constant value. At the low strain rates encountered in the cataract surgery simulation, the effect of strain rate, strain hardening, and thermal softening are vanished in the modified Johnson-Cook model. To implement the material formulation by using vumat subroutine of ABAQUS the user must provide, the yield stress of corneal tissue from experimental results.

## 3. RESULTS

Experimental results for two keratome velocities, i.e., 1mm/s and 2 mm/s, were carried out at four intraocular pressures ranging between 15 mm-Hg and 18 mm-Hg. Figure 4 demenstrates the results of the test when the keratome moved at the speed of 1 mm/s. As the intraocular pressure increases from 15 mm-Hg to 18 mm-Hg, force trajectory increases as well. Force increases until it reaches a peak at P as shown in Figure 4. This corresponds to the deformation of the corneal tissue before the incision of the tissue. Quickly after the peak, force declines from P to Q as a consequence of penetration. At Q, the edges of the keratome are in contact with the punched corneal tissue. The keratome continues to cut the tissue and push forward from Q to R. Consequently, force remains almost constant as time passes until the indentation reaches 1.6 mm at R, which coincides with the maximum width of keratome (3.2 mm) at this point. The soft tissue has been cut open by the full width of the keratome at R. From R to S, the keratome penetrates more into the cornea rather effortlessly through the cornea thickness, while force diminishes steadily and ultimately vanishes at T. The general behavior of experimental results in our research are similar to results of needle insertion into the soft gel in previous study [30].

Similarly, Figure 5 persents the test results for the keratome speed of 2 mm/s. The general behavior of Figures 4 and 5 are similar. We observe an 7.7% average increase in force when the speed doubled from 1 mm/s to 2 mm/s.

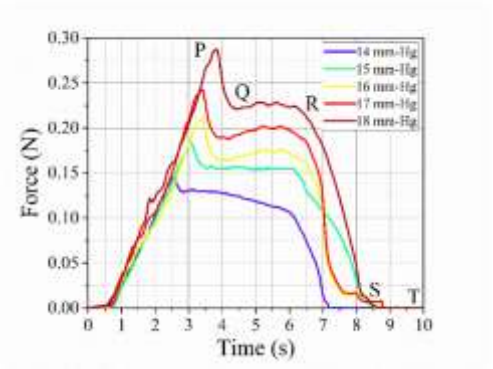


**Figure 4.** Experimental results for the 1-mm/s velocity with different pressure values

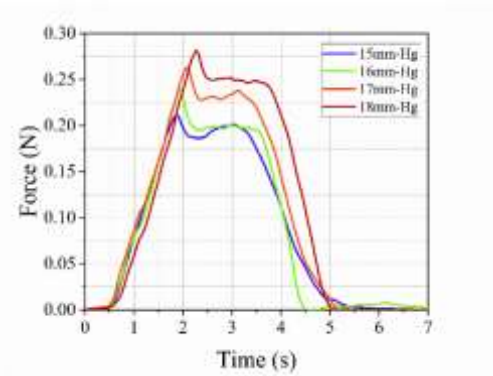


**Figure 5.** Experimental test results for the 2-mm/s velocity with different pressure values

Figure 6 compares incision force at four intraocular pressures for both velocities. The experimental results show that the keratome velocity does not affect force considerably. Also, the amount of force increase due to the faster velocity of 2 mm/s is diminished at higher intraocular pressures.

The FE model of the corneal tissue cutting process during cataract surgery operation was developed for four intraocular pressures between 15 mm-Hg and 18 mm-Hg.

The keratome velocity was set to 2 mm/s as the most common velocity during cornea cutting. Figure 7 shows four stages of keratome penetration into the corneal tissue for the intraocular pressure of 15 mm-Hg. Force exertion on the corneal tissue increases before incision as shown in Figure 7(a). Quickly thereafter the keratome tip penetrates into the corneal tissue and the edges of keratome remains in contact with the corneal tissue as shown in Figure 7(b). The keratome continues to cut open the corneal tissue by the full width of the keratome as shown in Figure 7(c). The keratome continues to penetrate into the cornea without further cutting as shown in Figure 7(d). The Von Misses stress of the corneal tissue resulting from the keratome penetration is expressed in MPa in a legend next to each figure.

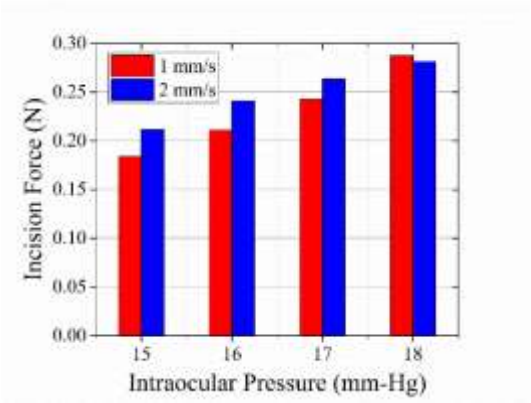


**Figure 6.** Comparison of the incision force at two keratome velocities of 1 mm/s and 2 mm/s

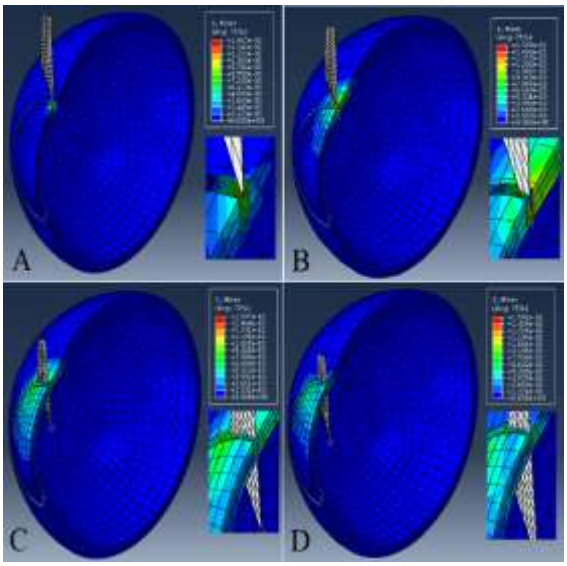


**Figure 7.** Von Misses stress during penetration; only half of the eye and keratome are drawn because of the eye symmertry about the prime meridian plane. A: Force exertion on the corneal tissue before incision; B: Keratome tip penetration into the corneal tissue; C: Corneal tissue cut open by the full width of the keratome; D: Continuation of keratome penetration into the cornea without further cutting

The resultant force on the keratome was calculated by ABAQUS and compared with the experimental results. Figures 8 presents the FEM results for the 2 mm/s velocity of the keratome motion for different intraocular pressures. The pattern of PQRST in experimental results in Figures 4 and 5 are observed in Figure 8.

The results of the experiments and the FEM are compared for the keratome velocity of 2 mm/s with two intraocular pressures of 15 mm-Hg and 18 mm-Hg as shown in Figures 9(a) and 9(b). These pressure values are chosen because they are the minimum and maximum common pressures used during cataract surgery operation by most surgeons. The pattern of experimental results and FE simulations are similar. Both experimental results and FE simulations show that the maximum force in Figure 9(b) is 24% bigger than that of in Figure 9(a) because of difference in intraocular pressures of 15 mm-Hg and 18 mm-Hg. Figures 9(c) and 9(d) show the errors of the FEM from the experimental results. In Figure 9(c), the root mean square and the maximum of the error are 0.009 N and 0.042 N, respectively. Similarly, in Figure 9(d), the root mean square and the maximum of the error are 0.007 N and 0.021 N, respectively.

## 4. DISCUSSION

A physics-based simulation of cataract surgery operation can improve surgical training by increasing the fidelity of

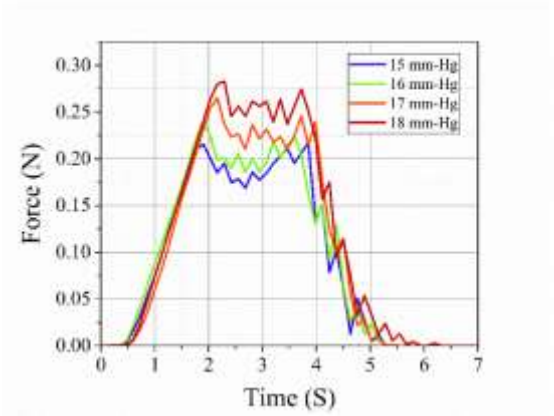


**Figure 8.** FEM results for the 2-mm/s velocity with different pressure values

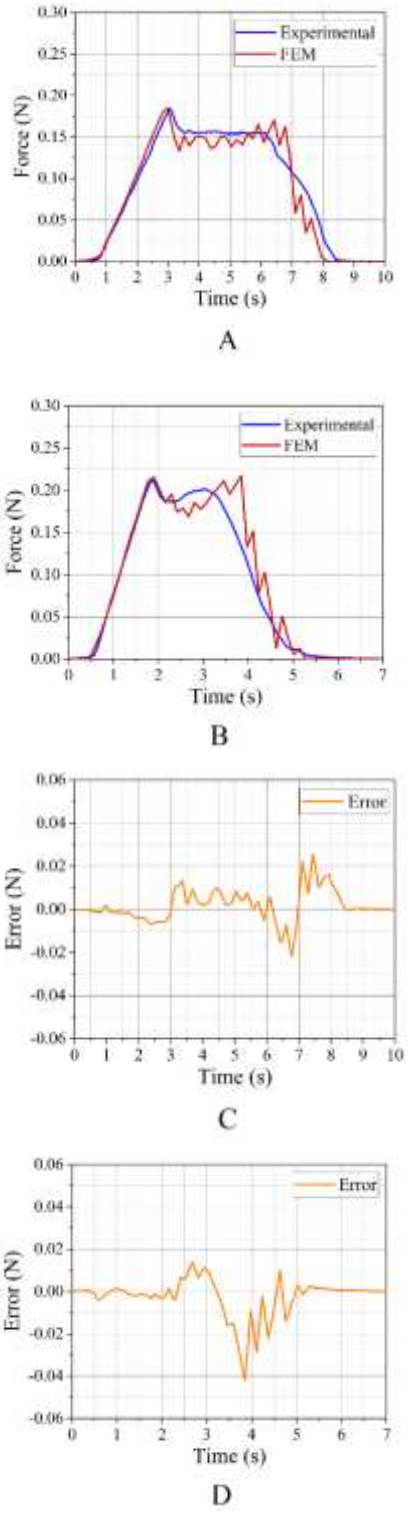


**Figure 9.** Experimental and FEM results. A: 15-mm-Hg pressure and the 2-mm/s velocity. B: 18-mm-Hg pressure and the 2-mm/s velocity. C: FEM difference from the experimental results for the 15-mm-Hg pressue and the 2-mm/s velocity. D: FEM difference from the experimental results for the 18-mm-Hg pressue and the 2-mm/s velocity

haptic simulators. Simulation of corneal tissue cutting process is an important part of cataract surgery training, but has not been adequately explored in the previous studies. For instance, recent studies in the field of refractive surgery [3, 4], and also previous studies on refractive surgery simulation [2, 37] modeled the geometry of corneal tissue before and after the surgical procedure without considering the cutting process. Similarly, researches in the field of projectile impact and trauma finite element simulation [17, 18] focused on the results of different parameters of the projectile affecting the intensity of injuries. Simulation of airbag injuries [20, 21] is similar to that of projectile impact injuries as both are not focused on the cutting process of the cornea. In fact, the mechanism and pattern of rupture in projectile and airbag studies are not under control. In other words, these studies aimed to predict the effects of different impact types on cornea to improve designs by creating a better protection. Therefore, the cutting procedure was not a key issue in such studies.

Research works in the field of needle insertion into a biological material [25, 33] have shown similar force-time patterns to the findings of this paper. The differences are the experimental setup, the surgical instrument, and the material properties of the soft tissue.

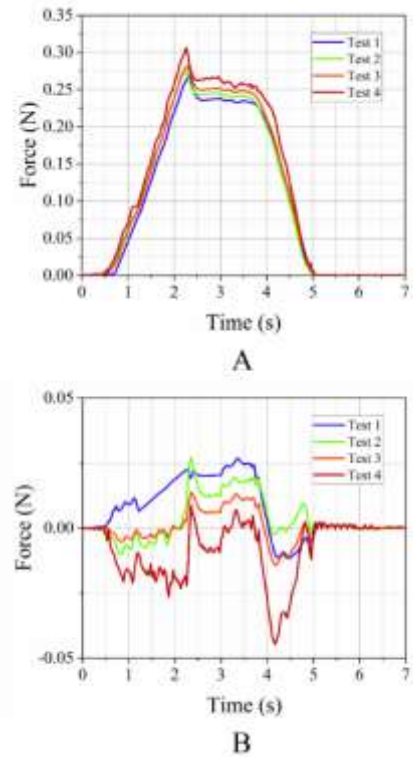


**Figure 10.** Repeatability of the test results. A: Test results for four ovine eyes (pressure of 18 mm-Hg and velocity of 2 mm/s). B: The difference of each test from the mean of all four tests

The repeatability of the experiments was investigated by four ovine eyes for each test. For example, Figure 10(a) shows the experimental results for the intraocular pressure of 18 mm-Hg and the keratome velocity of 2 mm/s. Figure 10(b) shows the test errors from the mean values. The force-time curves are close to each other with the root mean square of 0.013 N, 0.009 N, 0.006 N, and 0.014N for tests 1 to 4.

## 5. CONCLUSION

We designed and fabricated an experimental setup to measure force during the process of corneal tissue cutting in cataract surgery operation. We also developed a three-dimensional FE model for simulating keratome insertion into the corneal tissue. We validated this FE model by the experimental data at four intraocular pressures with the keratome velocity of 2 mm/s. The FE model included non-linear properties of the corneal tissue and a modified Johnson-Cook model for the cutting behavior during cataract surgery operation. The material behavior of this corneal tissue model is computationally inexpensive and can be used in real-time haptic simulators in order to better train surgeons and prepare them for handling potential complications of surgery. These simulations could also be useful to design better cataract surgery instruments. Real-time simulation of corneal cutting process by using haptic device is left for future work.

## 6. REFERENCES


1. Dhatt, G., Touzot, G. and Lefrançois, E., "Finite element method, Numerical methods series, London Hoboken, N.J., ISTE; Wiley, (2012), 600 p.
2. Pandolfi, A., Fotia, G. and Manganiello, F., "Finite element simulations of laser refractive corneal surgery", ***Engineering with Computers***, Vol. 25, No. 1, (2008), 15-24. DOI: 10.1007/s00366-008-0102-5.
3. Lehtikangas, O., Tarvainen, T., Kim, A.D. and Arridge, S.R., "Finite element approximation of the radiative transport equation in a medium with piece-wise constant refractive index", ***Journal of Computational Physics***, Vol. 282, No., (2015), 345-359. DOI: 10.1016/j.jcp.2014.11.025.
4. Sanchez, P., Moutsouris, K. and Pandolfi, A., "Biomechanical and optical behavior of human corneas before and after photorefractive keratectomy", ***Journal of Cataract & Refract Surgery***, Vol. 40, No. 6, (2014), 905-917. DOI: 10.1016/j.jcrs.2014.03.020.
5. Alastrue, V., Calvo, B., Pena, E. and Doblare, M., "Biomechanical modeling of refractive corneal surgery", ***Journal of Biomechanical Engineering***, Vol. 128, No. 1, (2006), 150-160. DOI: 10.1115/1.2132368.
6. Jessica R. Crouch, J.C.M., Earl R. Crouch III, "Finite element model of cornea deformation", in Medical Image Computing and Computer-Assisted Intervention - MICCAI. Vol., No. Issue, (2005 of Conference), 591-598.
7. Sinha Roy, A. and Dupps, W.J., Jr., "Effects of altered corneal stiffness on native and postoperative lasik corneal biomechanical behavior: A whole-eye finite element analysis", ***Journal of Refractive Surgery***, Vol. 25, No. 10, (2009), 875-887. DOI: 10.3928/1081597X-20090917-09.
8. Genest, R., "Finite element model of the chick eye to study myopia", ***Journal of Medical and Biological Engineering***, Vol. 33, No. 2, (2013). DOI: 10.5405/jmbe.1057.
9. Seven, I., Lloyd, J.S. and Dupps, W.J., "Differences in simulated refractive outcomes of photorefractive keratectomy (prk) and laser in-situ keratomileusis (lasik) for myopia in same-eye virtual trials", ***International Journal of Environmental Research and Public Health***, Vol. 17, No. 1, (2019). DOI: 10.3390/ijerph17010287.
10. Studer, H.P., Riedwyl, H., Amstutz, C.A., Hanson, J.V. and Buchler, P., "Patient-specific finite-element simulation of the human cornea: A clinical validation study on cataract surgery", ***Journal of Biomechanics***, Vol. 46, No. 4, (2013), 751-758. DOI: 10.1016/j.jbiomech.2012.11.018.
11. Cristobal, J.A., del Buey, M.A., Ascaso, F.J., Lanchares, E., Calvo, B. and Doblare, M., "Effect of limbal relaxing incisions during phacoemulsification surgery based on nomogram review and numerical simulation", ***Cornea***, Vol. 28, No. 9, (2009), 1042-1049. DOI: 10.1097/ICO.0b013e3181a27387.
12. Lapid-Gortzak, R., van der Linden, J.W., van der Meulen, I.J. and Nieuwendaal, C.P., "Advanced personalized nomogram for myopic laser surgery: First 100 eyes", ***Journal of Cataract & Refractive Surgery***, Vol. 34, No. 11, (2008), 1881-1885. DOI: 10.1016/j.jcrs.2008.06.041.
13. Sinha Roy, A., Dupps, W.J., Jr. and Roberts, C.J., "Comparison of biomechanical effects of small-incision lenticule extraction and laser in situ keratomileusis: Finite-element analysis", ***Journal of Cataract & Refract Surgery***, Vol. 40, No. 6, (2014), 971-980. DOI: 10.1016/j.jcrs.2013.08.065.
14. Lanchares, E., Calvo, B., Cristobal, J.A. and Doblare, M., "Finite element simulation of arcuates for astigmatism correction", ***Journal of Biomechanics***, Vol. 41, No. 4, (2008), 797-805. DOI: 10.1016/j.jbiomech.2007.11.010.
15. Besdo, S., Wiegand, J., Hahn, J., Ripken, T., Krüger, A., Fromm, M. and Lubatschowski, H., "Finite element study of the accommodation behaviour of the crystalline lens after fs-laser treatment", ***Biomedical Engineering / Biomedizinische Technik***, Vol., No., (2013). DOI: 10.1515/bmt-2013-4337.
16. R. B, B., Prabhu, G., S. Ve, R., Poojary, R. and Sundaram, S.M., "Investigation of deformation of the cornea during tonometry using fem", ***International Journal of Electrical and Computer Engineering***, Vol. 10, No. 6, (2020). DOI: 10.11591/ijece.v10i6.pp5631-5641.
17. Weaver, A.A., Kennedy, E.A., Duma, S.M. and Stitzel, J.D., "Evaluation of different projectiles in matched experimental eye impact simulations", ***Journal of Biomechanical Engineering***, Vol. 133, No. 3, (2011), 031002. DOI: 10.1115/1.4003328.
18. Gray, W., Sponsel, W.E., Scribbick, F.W., Stern, A.R., Weiss, C.E., Groth, S.L. and Walker, J.D., "Numerical modeling of paintball impact ocular trauma: Identification of progressive injury mechanisms", ***Investigative Ophthalmology & Visual Science***, Vol. 52, No. 10, (2011), 7506-7513. DOI: 10.1167/iovs.11-7942.
19. Koberda, M., Skorek, A., Kłosowski, P., Żmuda-Trzebiatowski, M., Żerdzicki, K., Lemski, P. and Stodolska-Koberda, U., "Extended numerical analysis of an eyeball injury under direct impact", Vol., No., (2021). DOI: 10.1101/2021.02.26.433021.
20. Uchio, E., Ohno, S., Kudoh, K., Kadonosono, K., Andoh, K. and Kisielewicz, L.T., "Simulation of air-bag impact on post-radial keratotomy eye using finite element analysis", ***Journal of Cataract & Refractive Surgery***, Vol. 27, No. 11, (2001), 1847-1853. DOI: 10.1016/s0886-3350(01)00966-x.

21. Uchio, E., Kadonosono, K., Matsuoka, Y. and Goto, S., "Simulation of air-bag impact on an eye with transsclerally fixated posterior chamber intraocular lens using finite element analysis", ***Journal of Cataract & Refractive Surgery***, Vol. 30, No. 2, (2004), 483-490. DOI: 10.1016/S0886-3350(03)00520-0.
22. S.P. DiMaio, S.E.S., "Needle insertion modeling and simulation", ***IEEE Transactions on Robotics and Automation***, Vol. 19, No. 5, (2003), 864 - 875. DOI: 10.1109/Tra.2003.817044.
23. Moustris, G.P., Hiridis, S.C., Deliparaschos, K.M. and Konstantinidis, K.M., "Evolution of autonomous and semi-autonomous robotic surgical systems: A review of the literature", ***The International Journal of Medical Robotics***, Vol. 7, No. 4, (2011), 375-392. DOI: 10.1002/rcs.408.
24. Misra, S., Reed, K.B., Douglas, A.S., Ramesh, K.T. and Okamura, A.M., "Needle-tissue interaction forces for bevel-tip steerable needles", ***Proc IEEE RAS EMBS Int Conf Biomed Robot Biomechatron***, (2008), 224-231. DOI: 10.1109/BIOROB.2008.4762872.
25. Oldfield, M., Dini, D., Giordano, G. and Rodriguez, Y.B.F., "Detailed finite element modelling of deep needle insertions into a soft tissue phantom using a cohesive approach", ***Comput Methods Biomech Biomed Engin***, Vol. 16, No. 5, (2013), 530-543. DOI: 10.1080/10255842.2011.628448.
26. Kong, X.Q., Zhou, P. and Wu, C.W., "Numerical simulation of microneedles' insertion into skin", ***Computer Methods in Biomechanics and Biomedical Engineering***, Vol. 14, No. 9, (2011), 827-835. DOI: 10.1080/10255842.2010.497144.
27. Assaad, W., Jahya, A., Moreira, P. and Misra, S., "Finite-element modeling of a bevel-tipped needle interacting with gel", ***Journal of Mechanics in Medicine and Biology***, Vol. 15, No. 05, (2015). DOI: 10.1142/s0219519415500797.
28. Podder, T.K., Sherman, J., Messing, E.M., Rubens, D.J., Fuller, D., Strang, J.G., Brasacchio, R.A. and Yu, Y., "Needle insertion force estimation model using procedure-specific and patient-specific criteria", Conference proceedings - IEEE engineering in medicine and biology society, Vol. 2006, No., (2006), 555-558. DOI: 10.1109/IEMBS.2006.259921.
29. Asadian, A., Kermani, M.R. and Patel, R.V., "A novel force modeling scheme for needle insertion using multiple kalman filters", ***IEEE Transactions on Instrumentation and Measurement***, Vol. 61, No. 2, (2012), 429-438. DOI: 10.1109/tim.2011.2169178.
30. van Veen, Y.R., Jahya, A. and Misra, S., "Macroscopic and microscopic observations of needle insertion into gels", ***Proceedings of the Institution of Mechanical Engineers, Part H***, Vol. 226, No. 6, (2012), 441-449. DOI: 10.1177/0954411912443207.
31. Jushiddi, M.G., Cahalane, R.M., Byrne, M., Mani, A., Silien, C., Tofail, S.A.M., Mulvihill, J.J.E. and Tiernan, P., "Bevel angle study of flexible hollow needle insertion into biological mimetic soft-gel: Simulation and experimental validation", ***Journal of the Mechanical Behavior of Biomedical Materials***, Vol. 111, No., (2020), 103896. DOI: 10.1016/j.jmbbm.2020.103896.
32. Yamaguchi, S., Tsutsui, K., Satake, K., Morikawa, S., Shirai, Y. and Tanaka, H.T., "Dynamic analysis of a needle insertion for soft materials: Arbitrary lagrangian-eulerian-based three-dimensional finite element analysis", ***Computers in Biology and Medicine***, Vol. 53, (2014), 42-47. DOI: 10.1016/j.compbiomed.2014.07.012.
33. Mahvash, M. and Dupont, P.E., "Mechanics of dynamic needle insertion into a biological material", ***IEEE Transactions on Biomedical Engineering***, Vol. 57, No. 4, (2010), 934-943. DOI: 10.1109/TBME.2009.2036856.
34. Elsheikh, A., Kassem, W. and Jones, S.W., "Strain-rate sensitivity of porcine and ovine corneas", ***Acta of Bioengineering And Biomechanics***, Vol. 13, No. 2, (2011), 25-36.
35. Mohammadi, S.F., Mazouri, A., Jabbarvand, M., Rahman, A.N. and Mohammadi, A., "Sheep practice eye for ophthalmic surgery training in skills laboratory", ***Journal of Cataract & Refractive Surgery***, Vol. 37, No. 6, (2011), 987-991. DOI: 10.1016/j.jcrs.2011.03.030.
36. Mohammadi, S.F., Mazouri, A., Rahman, A.N., Jabbarvand, M. and Peyman, G.A., "Globe-fixation system for animal eye practice", ***Journal of Cataract & Refractive Surgery***, Vol. 37, No. 1, (2011), 4-7. DOI: 10.1016/j.jcrs.2010.10.026.
37. Sinha Roy, A. and Dupps, W.J., Jr., "Patient-specific modeling of corneal refractive surgery outcomes and inverse estimation of elastic property changes", ***Journal of Biomechanical Engineering***, Vol. 133, No. 1, (2011), 011002. DOI: 10.1115/1.4002934.


## Persian Abstract


**چکیده**

مدلسازی برش sقرنیه یکی از اساسی‌ترین مسائل در توسعه شبیه سازهای آموزشی هپتیکی و ربات‌های جراحی می‌باشد. یک مدل المان محدود برای شبیه سازی مرحله برش قرنیه چشم گوسفند ایجاده شده و اعتبار بخشی آن توسط یک دستگاه تست که برای اولین بار ساخته شده است، صورت پذیرفته است. دستگاه تست، نیروها را در مرحله های مختلف برش قرنیه اندازه گیری می‌نماید. رفتار مکانیکی بافت قرنیه در هنگام برش به روش المان محدود مدلسازی شده است. تست های برش بر روی ۳۲ عدد چشم گوسفند در شرایط کاملا مشابه در بدن موجود زنده مورد تست قرار گرفته اند. نیرو با سرعت داده برداری ۲۰۰ هرتز ثبت شده است. تست در فشارهای داخلی مختلف قرنیه یعنی ۱۵ تا ۱۸ میلی متر جیوه و سرعت حرکت ۱ میلی متر بر ثانیه و ۲ میلی متر بر ثانیه انجام شده است. توسط مدل المان محدود رفتار غیر خطی بافت قرنیه چشم گوسفند مدلسازی شده است. قبل از اولین برش بافت قرنیه و ورود نوک ابزار برش داخل بافت نیرو افزایش می‌یابد. در لحظه ورود نوک ابزار به داخل بافت قرنیه به میزان ۱۲.۳ درصد در سرعت ۲ میلی متر بر ثانیه و به میزان ۱۹.۱ درصد در سرعت ۱ میلی متر بر ثانیه نیرو کاهش می یابد و بعد از آن نیرو تقریبا ثابت باقی می ماند. بعد از برش کامل که معادل با بیشترین عرض ابزار می‌باشد، نیرو از روی ابزار برداشته می‌شود و به سمت ناپدید شدن پیش می‌رود. نیروی برش قرنیه با تغییرات فشار در سرعت ۱ میلی متر بر ثانیه در بازه ۰.۱۸۳ نیوتن تا ۰.۲۸۷ نیوتن و در سرعت ۲ میلی متر بر ثانیه در بازه ۰.۲۱۱ نیوتن تا ۰.۲۸۱ نیوتن متغییر می‌باشد. مدل المان محدود نشان می‌دهد که بیشینه خطای پیش بینی شده توسط این مدلسازی برای سرعت ۲ میلی متر بر ثانیه برابر با ۰.۰۴۲ می باشد. خطای جذر میانگین مربعات بین مدلسازی المان محدود صورت گرفته و آزمایش های تجربی انجام شده برابر با ۰.۰۲۵ می باشد.